

The need for a taphonomic perspective in spatial analysis: formation processes at the Early Pleistocene site of Pirro Nord (P13), Apricena, Italy

D. Giusti^{a,*}, M. Arzarello^b

^a*Paläoanthropologie, Senckenberg Center for Human Evolution and Paleoecology, Eberhard Karls Universität Tübingen, Rümelinstr. 23, 72070 Tübingen, Germany*

^b*Dipartimento di Studi Umanistici, Università degli Studi di Ferrara, C.so Ercole I d'Este 32, 44100 Ferrara, Italy*

Abstract

Ever since their percolation from neighbour disciplines, archaeology has employed spatial statistics to unravel, at different scales, past human behaviors from scatters of material culture. However, in the interpretation of the archaeological record, particular attention must be given to disturbance factors that operate in post-depositional processes. In this paper, we answer the need for a specific taphonomic perspectives in spatial analysis by applying point pattern analysis of taphonomic alterations on the faunal and lithic assemblages from the Early Pleistocene site of Pirro Nord 13, Italy. The site, biochronologically dated between 1.3 and 1.6 Ma BP, provides evidence for an early hominin presence in Europe. The archaeological and paleontological deposit occurs as filling of a karst structure that is currently exposed. We investigated the distribution of the archaeological and paleontological assemblage, as well as the distribution of identified taphonomic features, in order to evaluate degree and reliability of the spatial association of the lithic artifacts with the faunal remains. Our results contribute to the interpretation of the diagenetic history of Pirro Nord 13 and support the stratigraphic integrity of the site.

Keywords: Spatial analysis, Point pattern analysis, Site formation processes,

*Corresponding author

Email address: domenico.giusti@uni-tuebingen.de (D. Giusti)

1. Introduction

2 Studies of site formation processes and spatial analyses have long recognized
3 the role of post-depositional factors in affecting the integrity of archaeological
4 assemblages (Hodder and Orton, 1976; Petraglia and Nash, 1987; Schick, 1984,
5 1986; Schiffer, 1972, 1983, 1987; Wood and Johnson, 1978). More recently, a
6 number of scholars have stressed the importance of establishing the degree of
7 disturbance to archaeological deposits to fully comprehend the archaeological
8 record (Dibble et al., 1997; Djindjian, 1999; Texier, 2000).

9 Beside geoarchaeological techniques, several archaeological and paleontolog-
10 ical methods are widely applied to characterize the processes involved in the
11 formation of an archaeological site and to assess any post-depositional ‘back-
12 ground noise’. Taphonomy moves from its original definition (Efremov, 1940)
13 to a wider conceptual framework, targeting vertebrate assemblages, as well as
14 taphonomic entities produced by human behaviour (Domínguez-Rodrigo et al.,
15 2011). Moreover and often in joint effort, from different spatial perspectives,
16 fabric analysis (Benito-Calvo and de la Torre, 2011; Bernatchez, 2010; Bertran
17 et al., 1997; Bertran and Texier, 1995; Domínguez-Rodrigo et al., 2014c; Leno-
18 ble and Bertran, 2004; McPherron, 2005; de la Torre and Benito-Calvo, 2013);
19 refitting analysis (López-Ortega et al., 2011; Sisk and Shea, 2008; Villa, 1982);
20 vertical (Anderson and Burke, 2008) and size distribution analysis (Bertran
21 et al., 2006, 2012; Petraglia and Potts, 1994) offer meaningful contributions in
22 the unraveling of site formation and modification processes.

23 The importance of spatial statistics in the interpretation of archaeological
24 sites has long been recognized (Hodder and Orton, 1976; Whallon, 1974). How-
25 ever, studies of spatial patterning mostly focus on the behaviour of past popula-
26 tions, assuming that scatters of material culture (if not disturbed) are reflections
27 of prehistoric activities. Moreover, distribution maps still rely mainly on visual
28 examinations and subjective interpretations (Bevan et al., 2013). On the other

29 hand, quantitative methods, adopted from neighbor disciplines since the early
30 1970s (see Hodder and Orton (1976); Orton (1982); and references therein),
31 continue to promote new impulses to archaeological spatial analyses and allow
32 for the characterization of spatial patterns by adopting a more formal, induc-
33 tive approach. Recent studies (Bevan and Conolly, 2006, 2009, 2013; Bevan
34 et al., 2013; Bevan and Wilson, 2013; Crema, 2015; Crema et al., 2010; Crema
35 and Bianchi, 2013; Eve and Crema, 2014; Orton, 2004), even acknowledging
36 post-depositional effects or research biases, have continued to adopt at different
37 scales (from intra-site to regional scales) improvements in spatial statistics to
38 unravel past human behaviors from scatters of material culture. Yet, only a
39 relatively limited number of scholars have applied spatial statistics to site for-
40 mation and modification processes analysis (Carrer, 2015; Domínguez-Rodrigo
41 et al., 2014b,a).

42 In this paper, we adopt a taphonomic perspective to spatial point pattern
43 analysis of the lithic and faunal assemblages from the Early Pleistocene site of
44 Pirro Nord 13, Italy (Arzarello et al., 2007, 2009, 2012; Arzarello and Peretto,
45 2010).

46 The site (P13) provides important contributions to the ongoing debate about
47 the first hominin occurrence in Europe (Carbonell et al., 2008; Crochet et al.,
48 2009; Despriée et al., 2006, 2009, 2010; Lumley et al., 1988; Parés et al., 2006;
49 Toro-Moyano et al., 2011, 2009, 2013). A ‘Mode 1’ lithic assemblage has been
50 identified in stratigraphic association with late Villafranchian/early Biharian
51 paleontological remains. Furthermore, the presence of the Arvicoline species
52 *Allophaiomys ruffoi* correlated to the *Mymomis savini* - *Mymomis pusillus* bio-
53 zone, allows for a biochronologically refined age of between 1.3 and 1.6 Ma,
54 making P13 one of the most ancient locality with human evidence currently
55 known in Western Europe (Lopez-García et al., 2015).

56 The paleontological and archaeological remains are preserved inside a com-
57 plex karst system, exposed and partially destroyed by mining activities of a
58 Mesozoic limestone quarry. The fissure P13 is a vertical fracture located at
59 the stratigraphic boundary between the Mesozoic limestone and the Pleistocene

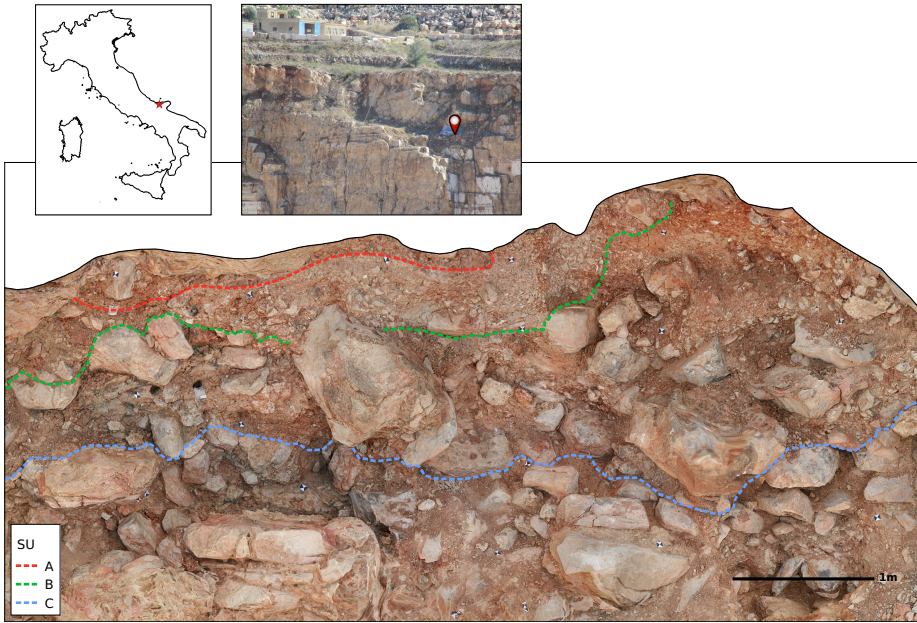


Figure 1: Location of the Pirro Nord (P13) site inside the Cave Dell'Erba quarry and view of the excavated area (2013), with marked sedimentary units.

60 calcarenite formation. The deposit of the fissure is, at the time of writing, more
 61 than 4 meters-thick. Four Sedimentary Units (SU's) have been distinguished on
 62 lithological basis. From the top to the bottom of the section, units A to D are
 63 characterized by sediments of clayey-sand of increasing thickness (Fig. 1). Unit
 64 A includes few coarse gravels and a very low number of paleontological and ar-
 65 chaeological remains. Unit B contains more gravels, while an abrupt increase in
 66 the number and dimension of clasts and large blocks of Pleistocene calcarenite is
 67 evident within units C and D. These last units show poor size sorting of angular
 68 and sub-rounded gravels, probably correlating to a low degree of reworking that
 69 took place during a short interval of time. We also record a significant increase
 70 in the number of fossils and artifacts.

71 As a residual component of a wider karst system, it is worthwhile to assess
 72 the degree of any potential post-depositional reworking of the archaeological
 73 and paleontological remains and to evaluate the stratigraphic integrity of the

⁷⁴ site.

⁷⁵ The main goal of our study is to use a taphonomic perspective in spatial
⁷⁶ data analysis, in order to evaluate degree and reliability of the spatial asso-
⁷⁷ ciation of the lithic artifacts with the faunal remains that were used for the
⁷⁸ biochronological dating of the site.

⁷⁹ By applying point pattern analysis of the spatial distribution of the lithic
⁸⁰ and faunal assemblages, we aim to

⁸¹ 1. investigate the processes involved in the formation of the Pirro Nord (P13)
⁸² deposit.

⁸³ A positive spatial association of the two types of find whould support the as-
⁸⁴ sumption, base on field observations, that the deposition of the archaeological
⁸⁵ and paleontological materials occured simultaneously, as result of subsequent
⁸⁶ mass wasting events.

⁸⁷ With the application of point pattern analysis to identified taphonomic fea-
⁸⁸ tures on the lithic and faunal assemblages, our ultimate objective is to

⁸⁹ 2. evaluate the degree of post-depositional disturbance of the site.

⁹⁰ Indeed, reworking and re-deposition processes could put in stratigraphic contact
⁹¹ materials from diverse provenience. The identification of taphonomic spatial
⁹² patterns allow us to model the spatial processes that produced them and thus
⁹³ propose a reconstruction of the agents involved in the formation and modifica-
⁹⁴ tion of the deposit.

⁹⁵ 2. Background

⁹⁶ With the authors' permission, we integrate in our study unpublished (Bag-
⁹⁷ nus, 2011) and published (Arzarello et al., 2012, 2014) data from previous tapho-
⁹⁸ nomic studies. A brief report is presented here.

⁹⁹ 2.1. *Taphonomy of macro vertebrate fossils*

¹⁰⁰ Taphonomic analysis (Bagnus, 2011) on macro vertebrate fossils evaluated
¹⁰¹ biostratinomic and diagenic processes and grouped faunal remains into different

¹⁰² sub-categories: three main taphorecords (TR's, *sensu* Fernández-López, 1987)
¹⁰³ are defined according to different stages of bone surface modifications by phys-
¹⁰⁴ ical and chemical agents (Tab. 1). Grouping was based mainly on weathering
¹⁰⁵ (Behrensmeyer, 1978; Díez et al., 1999; Kos, 2003; Torres et al., 2003), abra-
¹⁰⁶ sion (Behrensmeyer, 1991) and oxidation (Hill, 1982; López-González et al.,
¹⁰⁷ 2006; White, 1976; White et al., 2009), because these alterations prevail and are
¹⁰⁸ widespread across all the sedimentary units.

¹⁰⁹ Based on macroscopic observations of these main taphonomic features, fossils
¹¹⁰ from TR2 and TR3 are interpreted as re-deposited fossils: displaced bones along
¹¹¹ the sedimentary surface before burial; whereas fossils from TR1 are considered
¹¹² re-elaborated (*sensu* Fernández-López, 1991, 2007, 2011). The higher degree
¹¹³ of abrasion and the presence in the latter sub-group of multiple generations
¹¹⁴ of oxides, non uniformly distributed on the fossil, are explained with repeated
¹¹⁵ exhumations and dislocations of previously buried elements (López-González
¹¹⁶ et al., 2006).

¹¹⁷ Therefore, a hypothetical model of site formation processes has been pro-
¹¹⁸ posed: animals died close to the karst sinkhole and the action of heavy rains
¹¹⁹ transports sediments and partially articulated carcasses into the fissure. The
¹²⁰ rapid burial of fossils is confirmed by the general low degree of weathering. Karst
¹²¹ erosional processes are responsible for the very large percentage of fractured fos-
¹²² sils, as a result of the collapse of rock blocks from the vault. The TR1 group of
¹²³ fossils points to internal water-flows, reworking and transportation of already
¹²⁴ fossilized bones. Finally, manganese oxides that give the external widespread
¹²⁵ black color to all the fossils, stones and part of the lithic artifacts are products
¹²⁶ of the freatic water fluctuation.

¹²⁷ Although the taphonomic analysis definitely improved the interpretation of
¹²⁸ the P13 fossiliferous deposit, the interactions between bones and karst water flow
¹²⁹ have not been studied in relation to the spatial distribution and orientations of
¹³⁰ the skeletal elements.

¹³¹ Taking into account the inherent spatial properties of taphonomic processes,
¹³² we assume that taphogenic products (*sensu* Fernández-López, 2000) in space are

Table 1: Contingency table of taphorecords (reproduced from Bagnus, 2011).

SU	TR1	TR2	TR3	Total by SU
A	10	30	45	85
B	26	86	114	226
C	34	69	179	282
Total by TR	70	185	338	593

¹³³ not mutually independent and that entities which are close to each other, are
¹³⁴ likely to have followed the same genesis.

¹³⁵ Thus, in order to tackle our second objective, we analyze the spatial distribution
¹³⁶ of Fe-Mn oxides on the fossils, since the cause of their formation may derive
¹³⁷ from the action of circulating waters. Three ordinal degrees of oxidation (low,
¹³⁸ medium and high) are recognized, based on its aspect, intensity and extension.
¹³⁹ We assume that spatial aggregation of heavily-coated faunal remains (and con-
¹⁴⁰ sequently segregation from non-oxidized ones) is an indication of interactions
¹⁴¹ with karst water flow.

¹⁴² 2.2. *Taphonomy of lithic artifacts*

¹⁴³ The degree of natural alterations (thermal, tribological and chemical) of the
¹⁴⁴ lithic artifact surface, as a result of contact with the sediments, is a valuable
¹⁴⁵ index of integrity of the depositional context and it can usefully support spatial
¹⁴⁶ analysis in reconstructing both the past environmental conditions and the site
¹⁴⁷ formation processes (Burroni et al., 2002).

¹⁴⁸ According to a recent review of preliminary technological analyses (Arzarello
¹⁴⁹ et al., 2012, 2014), the lithic assemblage shows a general good state of preserva-
¹⁵⁰ tion. If we consider the degree of patination as a good indicator of the intensity,
¹⁵¹ and not necessary of the duration, of chemical processes to which the deposit
¹⁵² has been subjected (Burroni et al., 2002), artifacts undergo non-homogeneous
¹⁵³ interactions with chemical agents. Besides fresh artifacts, many of the speci-
¹⁵⁴ ments (35%) bear Fe-Mn coatings (Fig. 2a). Iron-manganese, as well as white

¹⁵⁵ superficial patina (5%), seems to equally affect artifacts of different flint raw
¹⁵⁶ materials, more readily on those with a porous structure (Fig. 2b).

¹⁵⁷ Macroscopic observations of tribological features on the assemblage reveal
¹⁵⁸ mint to sharp, not rounded, artifact ridges and edges. Post-depositional frac-
¹⁵⁹ tures affect 20% of the lithic material (Fig. 2c).

¹⁶⁰ No refittings were found, as it is reasonable to expect for materials in a
¹⁶¹ secondary context.

¹⁶² As particle size distribution of lithic assemblages has great implications in
¹⁶³ interpreting site formation processes (Bertran et al., 2012), systematic screen-
¹⁶⁴ washing of sediments was carried out in order to guarantee recovery of lithic
¹⁶⁵ debris, even though a very low percentage of small-size specimens has been
¹⁶⁶ noted. This result can be preliminary explained either as a function of the
¹⁶⁷ mode of knapping, which did not produce a lot of debris, or is more likely due
¹⁶⁸ to natural post depositional processes (washed-out effect of low energy agents),
¹⁶⁹ prior to final burial, possibly outside the karst fissure. Moreover, the dimensional
¹⁷⁰ analysis of the complete lithic assemblage (Fig. 2d) does not show sorting effects.

¹⁷¹ We analyse the spatial distribution of taphonomic features on the lithic
¹⁷² assemblage, considering that various natural mechanisms, disturbing the spa-
¹⁷³ tial arrangement of artifacts and sediments, will produce distinctive combina-
¹⁷⁴ tions of wear features on the surfaces of lithic artifacts (Burroni et al., 2002).

¹⁷⁵ As for the faunal assemblage, we focus the analysis on the distribution of Fe-
¹⁷⁶ Mn patinae. Three ordinal degrees of patination (absent, spotted and covering)
¹⁷⁷ are recognized, based on its presence and extension. In order to evaluate the
¹⁷⁸ impact of post-depositional processes at the site, we conduct independent and
¹⁷⁹ comparative taphonomic spatial analyses with the fossils remains.

¹⁸⁰ 3. Spatial data collection and sampling

¹⁸¹ Since 2007, systematic field investigations of the P13 fissure have been carried
¹⁸² out by the University of Ferrara (in collaboration with the Universities of Torino
¹⁸³ and Roma Sapienza, until 2010).

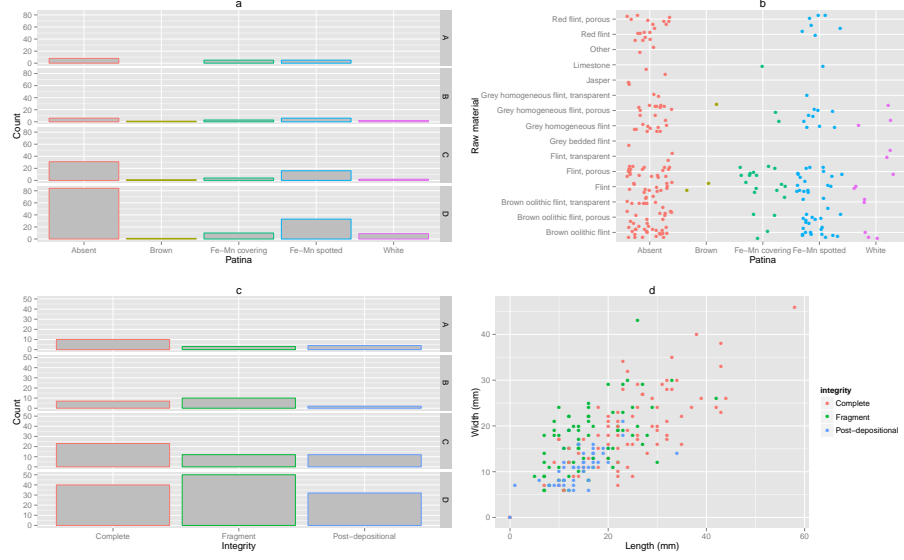


Figure 2: Frequency of patinae on the lithic assemblage (a) and their distribution on raw materials (b); frequency of fractures (c); scatterplot of artifact dimensions (d).

184 From the first excavation season, a grid of 1 square meter units has been set.
 185 Since 2010, the three-dimensional coordinates of the finds are recorded with a
 186 Total Station, which replaced the use of a water level. Orientation (dip and
 187 strike) of coordinated faunal remains (length ≥ 2 cm), geological clasts (length
 188 ≥ 5 cm) and all the lithic artifacts is estimated with a 45 degree of accuracy,
 189 which is not precise enough for detailed fabric analysis.

190 In order to avoid possible sampling issues in spatial data analysis due to the
 191 variation in the recording methods, we select subsets of the lithic and faunal
 192 collection, excluding SU's A and B, because they have been excavated prior the
 193 use of the Total Station.

194 Focusing on SU's C and D, we scale the windows of analysis according to
 195 the extension of excavated areas for each SU, excluding the presence of the
 196 large blocks of rock. We reduce in this way the impact of the Modifiable Area
 197 Unit Problem (MAUP) in point pattern analysis (Openshaw, 1996), especially
 198 insidious in this study due to the particular geological setting of the site. The

¹⁹⁹ analyzed areas of SU's C and D are respectively 4.34 m^2 and 5.82 m^2 .
²⁰⁰ During 6 years of excavations, more than 1600 of 2152 macro vertebrate
²⁰¹ fossils have been spatially recorded: 471 from SU C and 916 from SU D. How-
²⁰² ever, Bagnus (2011) conducted taphonomical analysis on fossils recovered dur-
²⁰³ing the 2007 to 2010 field seasons and only 593 of these are classified in one
²⁰⁴of the three taphorecords (Tab. 1). Our sample includes 135 coordinated el-
²⁰⁵ements of the 282 analyzed fossils from SU C. From the total number of 366
²⁰⁶lithic artifacts collected until the 2014 field season, 147 have been recorded with
²⁰⁷three-dimensional coordinates. Our sample includes 34 lithics from SU C and
²⁰⁸84 from SU D. From the micro mammal assemblage, we include in this study
²⁰⁹only the *Allophaiomys ruffoi* species. Of the 53 arvicoline teeth collected from
²¹⁰the screen-washed sediments, 49 have secure provenance attribution from SU B
²¹¹($n = 2$), C ($n = 14$) and D ($n = 33$) (Lopez-García et al., 2015). However, the
²¹²*A. ruffoi* point pattern does not represent the exact distribution of the remains.
²¹³Indeed, we randomly displaced ($r = 0.5$) each point indicating the provenience
²¹⁴of the sieved sediment.

²¹⁵ 4. Vertical distribution

²¹⁶ The vertical distribution of finds is a key factor in the analysis of site forma-
²¹⁷tion processes. Many processes can be well approximated by a ‘nearly’ normal
²¹⁸distribution. However, testing the appropriateness of this assumption is an es-
²¹⁹sential step in spatial data analysis. Strongly right skewed distribution would
²²⁰occur in case of a non-uniform vertical distribution of finds; thus requiring the
²²¹analysis to acknowledge the covariate effect of gravity in the observed spatial
²²²pattern.

²²³ The vertical distribution of finds within SU C is globally unimodal, roughly
²²⁴symmetric (slightly left skewed), in spite of some outliers (Fig. 3a). It ‘nearly’
²²⁵approximates the maximum-likelihood fitting of a normal curve (red line) with
²²⁶mean (μ) = -1.53 m and standard deviation (σ) = 0.27 m . However the Shapiro-
²²⁷Wilk normality test reject the null hypothesis of a gaussian distribution ($p -$

228 value = 0.0005213). On the other hand, the Q-Q plot (Fig. 3b) shows deviations
229 from the theoretical normal distribution (red line) between one (68.27% of the
230 sample) and two (95.45%) standard deviations from the mean. The S-shaped
231 empirical distribution recalls its left skew.

232 The global vertical distribution of finds resemble that of the faunal assem-
233 blage, due to the weight of the latter on the sample data ($n = 471$). The
234 distribution of the lithic artifacts is more left skewed, while the small sample
235 of micromammals follows a multimodal distribution with a prominent peaks
236 at -1.2 m (Fig. 3a). Although the difference in size of the two samples, it is
237 worth notice that the mean value of the vertical distribution of the *A. ruffoi*
238 species is very close to that of the lithic artifacts (Welch Two Sample t-test
239 $p - value = 0.5803$).

240 The vertical distribution of finds in SU D is globally unimodal, slightly left
241 skewed, with one peak at -2.10 m and no outliers (Fig. 3c). Although the
242 distribution is close to the best fitting normal curve (red line) with $\mu = -2.34$ m
243 and $\sigma = 0.33$ m, the Shapiro-Wilk test rejects the hypothesis of normality
244 ($p - value = 2.497e - 12$). The Q-Q plot (Fig. 3d) shows a more dispersed
245 distribution respect to the former one. Its steeper line follows the theoretical
246 normal distribution within one standard deviation from the mean (68.27% of
247 the sample).

248 Compared with the global distribution, the vertical distribution of lithic
249 artifacts slightly skews to the right. Nevertheless, the Shapiro-Wilk test fails
250 to reject the normality hypothesis ($p - value = 0.2742$). On the other hand,
251 the micromammals distribution is multimodal and slightly shifted to the right
252 (Fig. 3c). Its mean (-2.284 m) is quite close to the mean of the lithic sample
253 (-2.423 m). However, the Welch t-test rejects the hypothesis of two equal sam-
254 ple means ($p - value = 0.01414$). If we cannot state that the two distributions
255 have the same mean, we remark the highest density of both the assemblages at
256 around -2.5 m.

257 As for the vertical distribution of the identified taphonomic features on the
258 lithic and faunal assemblages, figures 4a,b illustrate the overall distribution of

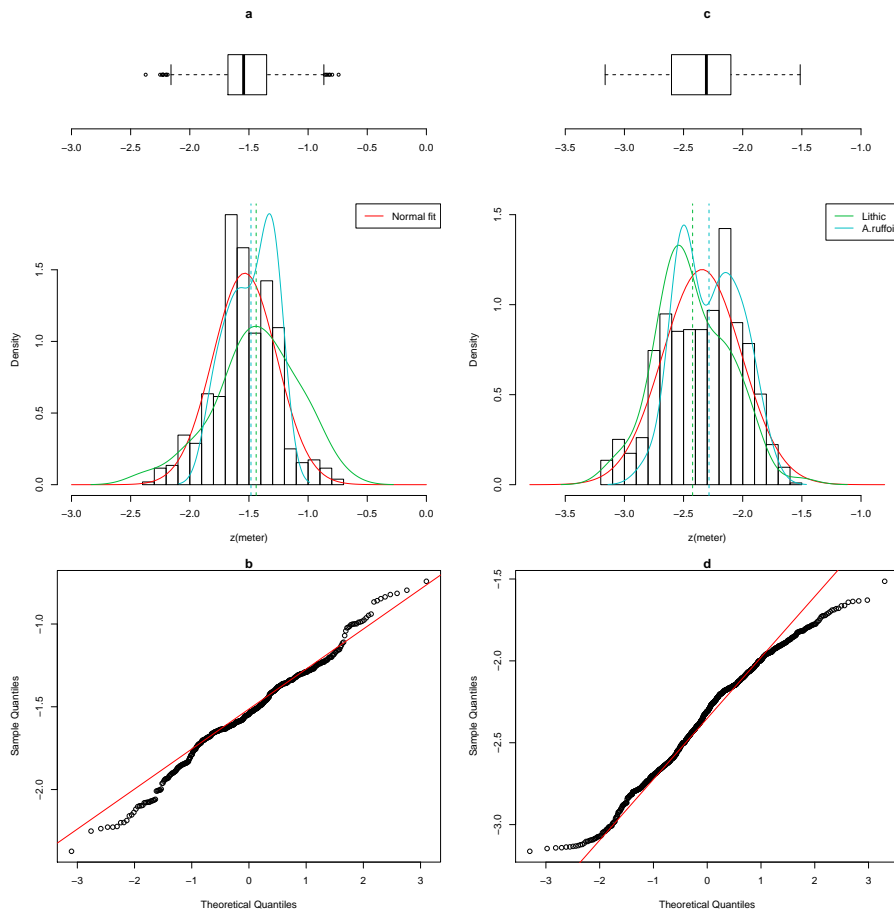


Figure 3: Vertical distribution of finds in SU's C (a,b) and D (c,d).

259 patinae on the lithic artifacts, across SU's C and D. The histogram shows the
260 increasing number of finds between the two sedimentary units. This trend is
261 reflected as well in the rise of Fe-Mn patinated artifacts (41% in SU C and 45% in
262 SU D), compared to non-patinated ones (respectively 50% and 48%). The kernel
263 density estimation (blue and green lines) shows a slightly higher occurrence of
264 patinated artifacts at the lower part of the sequence (below -2.5 m), whereas in
265 SU C (up to -2 m) there is no evident preference in the vertical distribution of
266 patinae. The higher density of patinated artifacts, linked to the concentration
267 of lithics observed in figure 3c at about -2.5 m, can be localized in a restricted
268 spot at the bottom right corner of the excavated area (Fig. 4a).

269 Restricting the analysis to SU C, the vertical distribution of coordinated
270 macro vertebrate fossils analized by Bagnus (2011) spans 71% of the elevation
271 range of the complete assemblage from the same SU. However, beeing only the
272 29% of the population, we acknowledge that our sample cannot be considered
273 representative.

274 The densities of the low and medium rate of oxides resemble the general dis-
275 tribution (Fig. 4c,b). Low values follow a 'nearly' normal distribution (Shapiro-
276 Wilk normality test $p-values = 0.2186$). The density of high oxidized remains
277 (54% of the sample) draws a left skewed distribution, with a peak at about
278 -1.3 m; whereas fossils with a medium degree of oxides are skewed to the right.
279 However there is no clear preference for oxides to occur deeper in the sequence.
280 The mean values are very close to each other and lower values of oxides are
281 more dense at the bottom of the SU.

282 As for the distribution of the three taphorecords, the prominent peak of TR1
283 at -1.6 m (Fig. 4f) contrast with a more distributed and mixed distribution of
284 the second and third group of fossils. However, the very low frequency of TR1
285 ($n = 9$) limits further analyses.

286 Although our study is constrained by the small sample of fossils and by its
287 limited spatial extension to SU C, the analysis of the vertical distribution of Fe-
288 Mn oxides in the faunal and lithic assemblages does not show any clear global
289 pattern. Indeed, even taking into account the localized cluster of artifacts at the

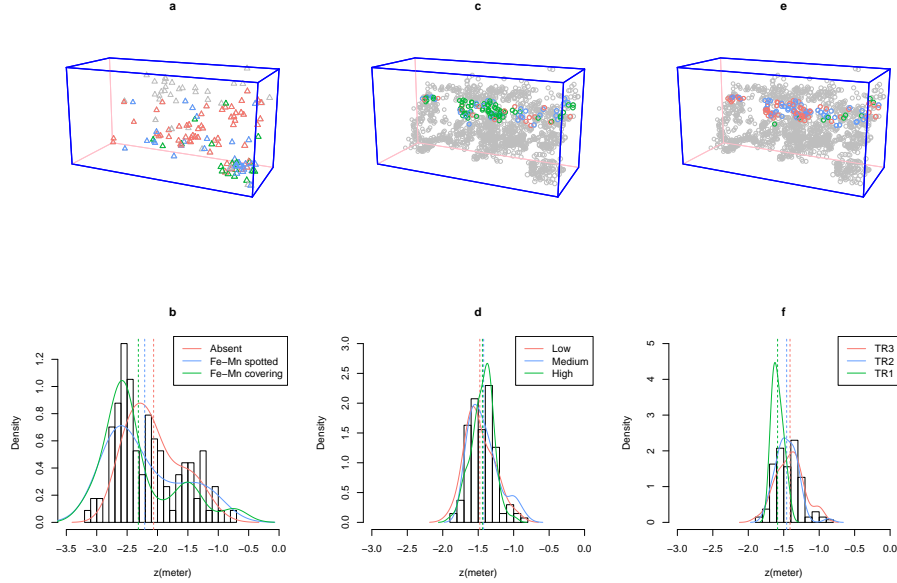


Figure 4: 3D and vertical distributions of Fe-Mn patinae on the lithic assemblage from SU's C and D (a,b); oxides (c,d) and taphorecords (e,f) from the faunal sample.

290 very bottom of SU D (Fig. 4a), the process responsible for the distribution of
 291 Fe-Mn oxides seems to operate indistinctly through the complete stratigraphic
 292 sequence, with no explicit preference for lower elevations.

293 With no evidence for strong right skewed distributions of finds in SU's C
 294 and D, we have reasons to exclude the covariate effect of gravity in the observed
 295 spatial pattern. The subsequent point pattern analyses are directed to the study
 296 of the 2D spatial distribution of fossils, lithics and their taphonomic status.

297 5. Point pattern analysis

298 The observed patterns of the archaeological and paleontological remains
 299 within SU's C and D, as well as the patterns of taphonomic features recog-
 300 nized on them, have been treated as realizations of spatial point processes, i.e.
 301 site formation and modification processes.

302 Indeed, a spatial point pattern is generally defined as the location of events

303 generated by a point process, operating simultaneously at different scales: a
304 first-order global scale and a second-order local scale (Bailey and Gatrell, 1995).
305 The former results from the frequency (density) of events within a bounded
306 region; the latter results from spatial dependency between points, e.g. from
307 a tendency for values of the process at nearby locations to interact with each
308 other. Three different types of interpoint interaction are possible: random (or
309 Poisson); regular and cluster. Regular patterns are assumed to be the result of
310 inhibition processes, while cluster patterns are the result of attraction processes.
311 Therefore, two main issues of interest are explored by spatial point pattern
312 analyses: the distribution (density) of entities in space and the existence of
313 possible interactions between them (Ord, 1972).

314 First-order effect in the observed point-pattern is generally non-parametrically
315 evaluated by means of kernel density estimation (Diggle, 1985). As an average
316 density of points in the study region, intensity informs about uniform or inho-
317 mogeneous distribution of events.

318 Multiple scales of second-order patterning and the probability of a stochastic
319 occurrence are explored by the Ripley's K summary function (Ripley, 1976,
320 1977) and derivates, for both univariate and bivariate point patterns. The K
321 function is designed to identify the relative aggregation and segregation of point
322 data at different scales. The univariate $K(r)$ function measures the expected
323 number of events found up to a given distance r around an arbitrary event.
324 By comparing the estimated value $\hat{K}(r)$ to its theoretical Complete Spatial
325 Randomness (CSR) value, it is possible to assess what kind of interaction exists
326 between events. The bivariate function, or cross-type $K_{ij}(r)$ function seeks to
327 evaluate, at each distance r , the spatial relation between two types ij of observed
328 events. In this case, the definition of the null hypothesis uses a randomization
329 technique of either the location of one of the types (random shift hypothesis),
330 or the type itself of the event at each point, preserving the original location
331 (random labeling hypothesis) (Goreaud and Pélissier, 2003). The former aims to
332 evaluate the spatial relationship between patterns of two independent processes,
333 while the latter assumes the same process in determining the pattern for different

334 types.

335 Especially in small dataset, the estimation of correlations between points is
336 biased by edge effects, arising from the unobservability of points outside the
337 window of analysis. In order to reduce that bias, we implement here Ripley's
338 isotropic edge correction (Ripley, 1988; Ohser, 1983).

339 Monte Carlo simulations (Robert and Casella, 2004) are used to generate
340 pointwise critical envelopes of random expected values for the null hypothe-
341 ses, providing an adequate level of statistical significance. We choose a small
342 significance level ($\alpha = 0.01$ obtained with 199 simulations), due to the higher
343 possibility to commit a Type 1 error by testing our hypotheses. Values of the em-
344 pirical distribution (black solid line) are plotted against the theoretical Poisson
345 distribution (red dotted line) and the simulated global envelope of significance
346 (grey area). For $K(r)$, when the solid line of the observed distribution is above
347 or below the shaded grey area, the pattern is significantly clustered (points are
348 closer together than would be expected for a complete random pattern) or dis-
349 persed. For $K_{ij}(r)$, the benchmark value πr^2 is consistent with independence
350 between the points of type i and j , and does not imply a Poisson distribution.

351 *5.1. Formation processes*

352 In order to investigate the processes involved in the formation of the Pirro
353 Nord deposit, we provisionally assume the deposition of each sedimentary unit
354 to be the result of mass wasting events filling the fissure and resulting in the
355 distribution of fossils and artifacts independently of each other.

356 To test the appropriateness of our working assumption, we first analyse the
357 overall distributions of finds, treated as univariate point patterns. Applying a
358 set of exploratory statistics, we aim to determine the nature of the depositional
359 processes, e.g. if they raise in- or homogeneous distributions. Then, we analyse
360 the relative patterns of the faunal and lithic assemblages from SU's C and D.
361 In this case, we treat the two distributions as multitype point patterns.

362 The intensity of the lithic and faunal assemblages is non-parametrically es-
363 timated by first performing a Gaussian smoothing kernel of their distributions,

364 for both SU's. Likelihood cross-validation bandwidth, which assumes an in-
365 homogeneous process, is selected for each pattern. Edge correction is applied
366 using the method of Diggle (1985). Then, Berman's Z_2 test is used to deter-
367 mine whether or not the intensity depends on a spatial covariate Z , assuming
368 that the spatially varying (inhomogeneous) intensity is a function of Z . Thus,
369 in order to measure the strength of dependence on the covariate, we use the
370 Receiver Operating Characteristic (ROC) curve. Spatially adaptive smoothing,
371 nearest-neighbour density and scan tests have been used in order to assess for the
372 evidence of hot spots in the intensities of the unmarked point patterns. Estima-
373 tions of the $K(r)$ and the Kaplan-Meier corrected empty-space $F(r)$ functions
374 provide further methods for the interpretation of the distributions.

375 Multitype summary functions are used in the analysis of the dependence
376 between points of the two assemblages. In this case, our main research question
377 is whether different types of finds have the same spatial distribution. The cross-
378 type $K_{ij}(r)$ function and the Kaplan-Meier corrected nearest-neighbour $G_{ij}(r)$
379 function are used to estimate the association between points of type i and j ,
380 for any pair of types of finds. Positive spatial correlation between the two
381 types of finds would suggest that lithic artifacts are more likely to be found
382 close to fossils than would be expected for the hypothesis of *independence*. It
383 would confirm the field observations about their close stratigraphic association
384 and further support our hypothesis that both patterns are the realization of
385 one depositional process. On the other hand, segregation of the two patterns
386 is equivalent to variation in the probability distribution of types. Segregation
387 could be interpreted as the expression of preferential/differential depositional
388 processes. In this case, more detailed analyses would be necessary.

389 *5.2. Post-depositional processes*

390 In order to evaluate the degree of post-depositional disturbance of the de-
391 posit, the spatial dependence of observed taphonomic features is assumed to
392 be the expression of a related diagenetic process. Measured phenomena that
393 are closer together in space, tend to be more related than those further apart

394 (Tobler, 1970).

395 Like in applications of point pattern analysis in spatial epidemiology (Diggle,
396 2003; Gatrell et al., 1996), we distinguish between *cases* and *controls*. The
397 distribution of cases of a certain taphonomic alteration can be regarded as the
398 realization of a diagenetic point process, whereas controls points refer to non-
399 altered remains. In a conditional analysis of a spatial case-control study the
400 locations are fixed covariates, and the taphonomic status is treated as a random
401 variable. The simplest null model (*random labelling*) is that the taphonomic
402 status of each find is random, independent and with constant risk of occurrence.

403 Spatial correlations of diagenetic alterations on the lithic and faunal assem-
404 blage are explored by the $K_{ij}(r)$ function, random labelling the pair case/control
405 of Fe-Mn oxidation. We assume in this case that an independent process (karst
406 water circulation), subsequent to the initial event responsible for the accumu-
407 lation of the finds in each SU, determined their preservation status. Positive
408 deviations from the null hypothesis, suggest that cases are more likely to be
409 found close to controls than would be expected if their status was randomly de-
410 terminated. On the other hand, negative deviations would indicate segregation
411 between cases and controls. Thus, it would suggest that the action of post-
412 depositional water-related processes could have locally reworked the original
413 distribution, determining the altered status of the remains.

414 All the spatial analyses were performed using the *spatstat* package (Baddeley
415 et al., 2015) in R statistical software (R Core Team, 2015).

416 A repository containing a compendium of data, source code and text is
417 archived at the DOI: 10.5281/zenodo.51764

418 **6. Results**

419 *6.1. Formation processes*

420 Figures 5c,d show the smoothing kernel estimation of the faunal assemblage
421 intensity respectively in SU's C and D. Lithic artifacts and micromammals re-
422 mains of the *A. ruffoi* species are superimposed on it. The visual assessment of

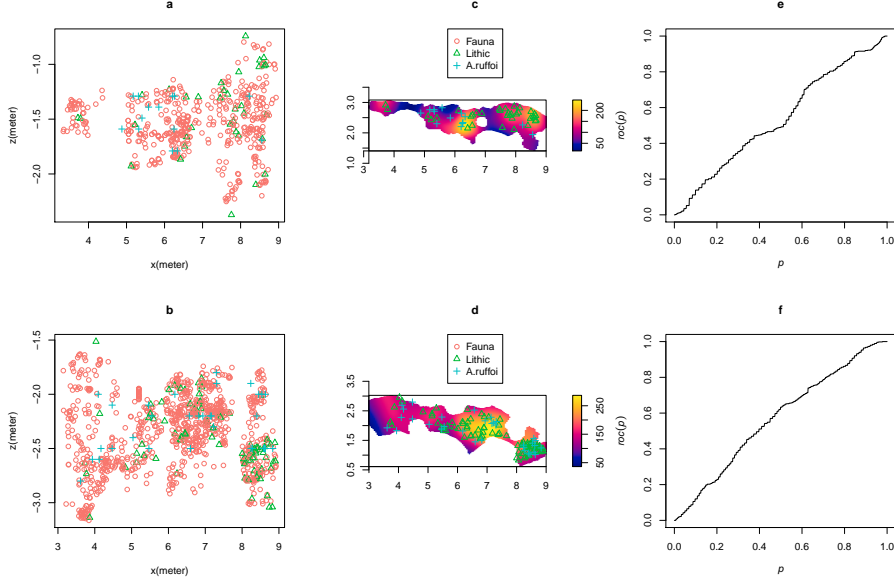


Figure 5: Scatterplot of finds from SU's C (a) and D (b); Smooth density estimation of the faunal assemblage and distribution of lithic artifacts and *A.ruffoi* remains in SU's C (c) and D (d); ROC curves for the covariate x coordinate in SU's C (e) and D (f).

423 the plot suggests positive spatial association between the three types of finds.
 424 Higher intensities in the distributions are evident at specific values of the x co-
 425 ordinate ($6 < x < 7$ and $8 < x < 9$), in both the sedimentary units. Yet,
 426 a concentration of artifacts, already observed in figure 3c and 4a,b, is evident
 427 at the lower right corner of SU D (Fig. 5e). Such higher densities of finds
 428 are clearly showed as well in the scatterplots of the projected third coordinate
 429 (Fig. 5a,b). Notably, the thickness of the sedimentary unit cannot be accounted
 430 to be responsible for those hot spots with higher density of finds. Neither the
 431 apparent inhomogeneous intensities along the x axes is supported by the ROC
 432 curves (Fig. 5e,f). Even if Bermans's Z_2 tests suggest significant evidence of de-
 433 pendence on the x covariate, the ROC curves show that it does not have strong
 434 discriminatory power.

435 Figures 6a,d show the resulting p-values of likelihood ratio scan test statistic.
 436 The test detects differences in the densities of the distributions, showing zones

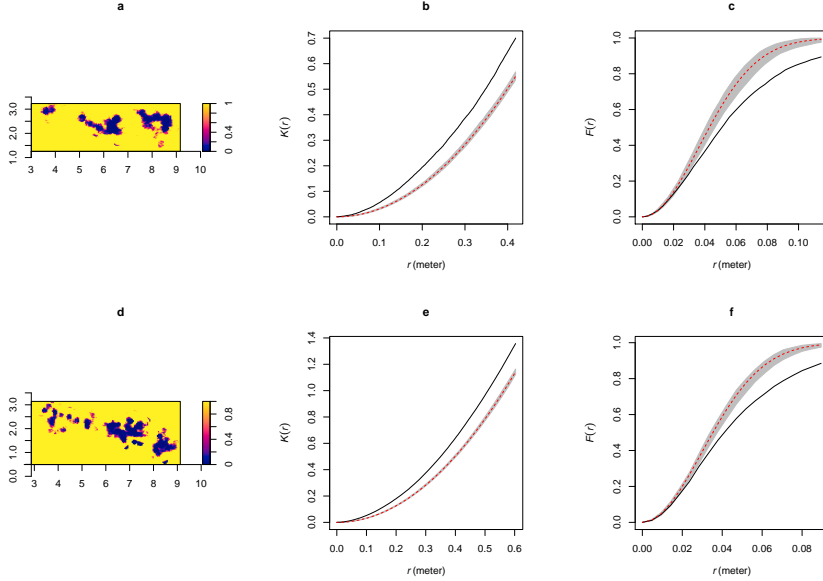


Figure 6: p-values of the likelihood ratio scan test, with logarithmic colour scale, for SU's C (a) and D (d); pointwise envelopes of the homogeneous $K(r)$ and $F(r)$ functions for unmarked finds from SU's C (b,c) and D (e,f).

437 with high abundance of finds. The estimated homogeneous $\hat{K}(r)$ and $\hat{F}(r)$
 438 functions are consistent with this result. For both SU's C (Fig. 6b,c) and D
 439 (Fig. 6e,f) they suggest strong deviation from the null hypothesis of CSR towards
 440 aggregation, at any scale.

441 In analysing a point pattern, it is confounding and it may be impossible
 442 to distinguish between clustering and spatial inhomogeneity (Baddeley et al.,
 443 2015). Given the context of the site, and the results of our non-parametric
 444 analyses, we proceed considering the distributions of finds as the results of clus-
 445 ter homogeneous processes. The bivariate version of the homogeneous $K_{ij}(r)$
 446 and $G_{ij}(r)$ function allow us to statistically test the hypothesis of aggregation
 447 between the types of remains.

448 In figure 7, the top line of panels (a,b,c) shows the ordinary estimations of
 449 the K function for the three types of finds (Fauna, Lithic and *A. ruffoi*) from
 450 SU C. Panel 7a resembles figure 6b and indicates statistical significant clustering

of the faunal remains for any values of r . The lithic assemblage shows as well a significant cluster tendency, for $r > 0.1$, while it fails to reject the null hypothesis of CSR for lower values. Instead, the estimated $\hat{K}(r)$ for the micromammals shows aggregation, but, for all values of r , we cannot state that the distribution is not random. This result might reflect the random displacement applied to the micromammal point pattern.

The middle and bottom lines of panels in figures 7 show estimations of the homogeneous cross-type K and G functions for all pairs of type i and j . Interestingly, figure 7d suggests positive spatial correlation between lithic and faunal remains at any values of $r > 0.05$. The corresponding $G_{ij}(r)$ function measured the cumulative distance from each point of type i (Lithic) to the nearest point of type j (Fauna). It shows (Fig. 7g) that the nearest-neighbour distances are significantly shorter than expected, but we cannot reject the hypothesis of independence between fossils and artifacts. However, the short scale of the function suggest that any artifacts is surrounded by fossils. This result statistically confirms the stratigraphic association of artifacts and fossils, previously based on field observations. On the other hand, deviations between the $\hat{K}_{ij}(r)$ function and the benchmark πr^2 suggest segregation between lithics and *A. ruffoi* specimens, but the hypothesis of independence between the two types is more significant (Fig. 7e,h). Conversely, the small mammal assemblage is closer to the rest of the fossils than expected for independent distributions, for $r > 0.2$. For lower values of r , the K and G functions fail to reject the hypothesis of independence.

The top line of panels in figure 8 (a,b,c) shows estimations of the $K(r)$ function for the three types of finds from SU D. Panel 8a confirms the same clustering trend of the faunal assemblage. Analogous to the distribution of finds from SU C, the global pattern is mostly weighed on the faunal assemblage (Fig. 6e). Conversely, in SU D the distribution of lithics shows stronger significant clustering for $r > 0.1$. Again, the resulting $\hat{K}(r)$ for the micromammal assemblage suggests a statistically insignificant aggregation tendency for all values of r , but $0.4 < r < 0.5$. In contrast to the previous result, estimations of the $K_{ij}(r)$

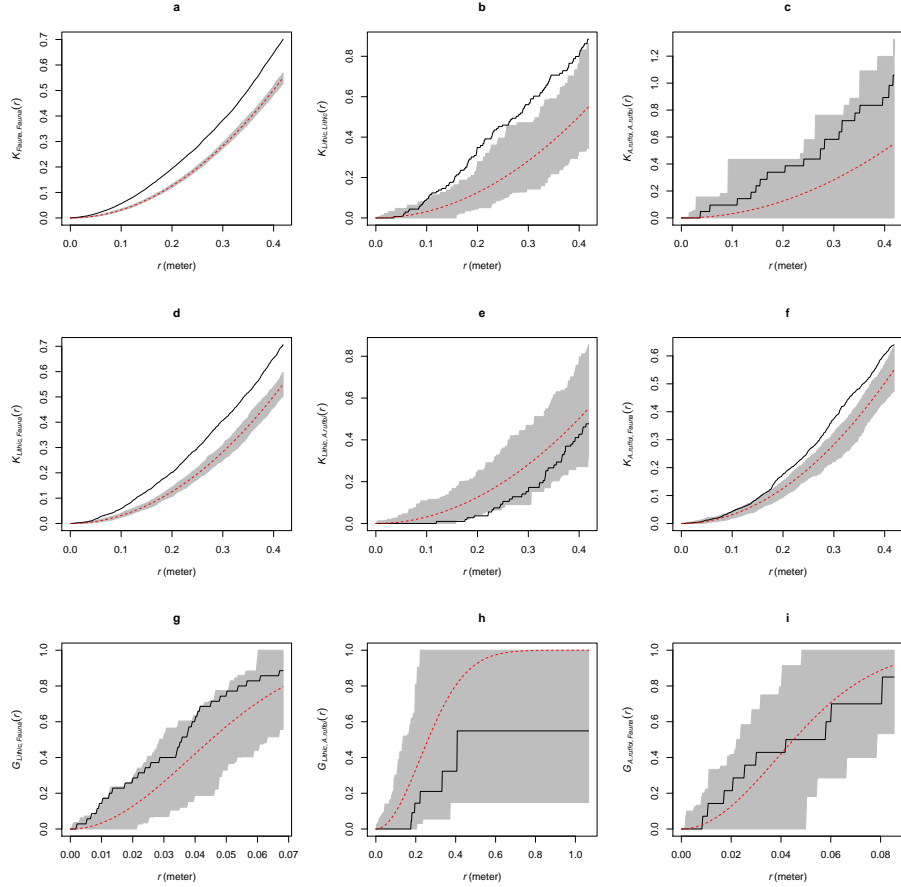


Figure 7: Pointwise envelopes of the homogeneous cross-type $K_{ij}(r)$ and $G_{ij}(r)$ functions for all pair of type i and j in SU C.

482 function support significant positive correlation between the lithic artifacts and
483 the *A. ruffoi* remains (Fig. 8e). Thus, they occur closer than expected in the
484 case of independent distributions. Panel 8f shows the same positive correlation
485 also between micro and macro mammals for $r > 0.2$. The panels 8d,g show
486 as well significant positive aggregation between lithics and fossils for values of
487 $r > 0.1$. In addition, the estimated $\hat{G}_{ij}(r)$ function offers a closer view of the
488 distribution. For values of $r < 0.1$, it fails to reject the hypothesis of indepen-
489 dence.

490 *6.2. Post-depositional processes*

491 To achieve our second objective, namely to evaluate the degree of post-
492 depositional disturbance of the deposit, we first analyzed spatial distribution of
493 oxides on the lithic and faunal assemblages independently, then we moved to a
494 comparative analysis. We are particularly interested in the spatial distribution
495 of Fe-Mn oxides (cases) compared with the absence of them (controls).

496 Figure 4a does not suggest segregation of patinated and non-patinated lithics.
497 If we perform random labeling of the presence of Fe-Mn (spotted and covering)
498 with its absence in both the stratigraphic units, the outputs of the cross-type
499 function (Fig. 9a, b) show that the observed altered artifacts are, with a 0.01
500 level of significance, randomly and independently located in SU C. The pos-
501 tive discrepancy between the estimated $\hat{K}_{ij}(r)$ and the benchmark πr^2 indicate
502 aggregation of cases and controls, but it lies within the grey envelope of the
503 *random labeling* hypothesis. Conversely, patinated and non-patinated lithics in
504 SU D appear to be closest to each other than expected for the null hypothesis.
505 In this unit the observed $\hat{K}_{ij}(r)$ function over-exceeds the envelope at values of
506 $r > 0.4m$, hence it indicates statistically significant aggregation. Such pattern
507 statistically confirms the visual assessment of figure 4a. Consequently, oxidized
508 and non-oxidized artifacts most probably occur in SU D well aggregated in
509 space, while their aggregation is not statistically significant in the above unit.

510 We could not compare the oxidation patterns between lithics and fossils from
511 SU D, because the taphonomic analysis of Bagnus (2011) did not include fossils

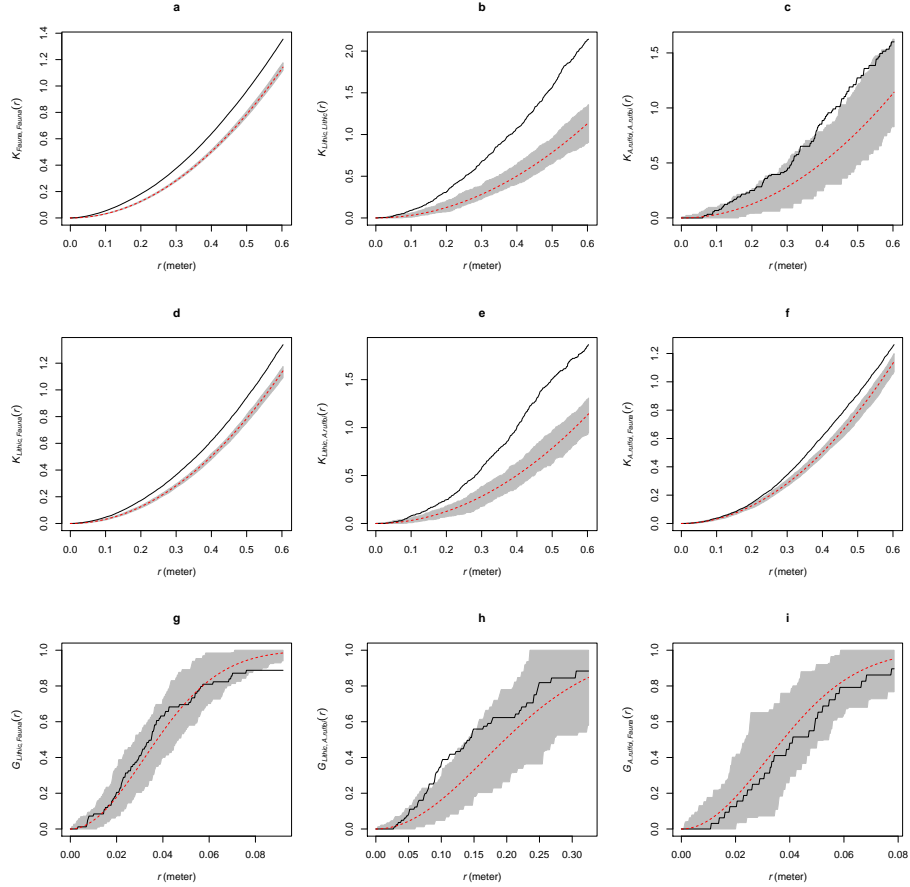


Figure 8: Pointwise envelopes of the homogeneous cross-type $K_{ij}(r)$ and $G_{ij}(r)$ functions for all pair of type i and j in SU D.

512 from this unit. Thus, we focused our analysis on SU C.

513 The distribution map (Fig. 4c) does not suggest any evident pattern. When
514 we apply random labelling of the absence of oxidation with the medium and high
515 degrees of its presence, the output of the bivariate $K_{ij}(r)$ function shows a seg-
516 regation tendency between them, but it is not statistically significant. (Fig. 9c).
517 A random and independent distribution of oxides is more plausible.

518 Finally, figure 9d shows the result of the $K_{ij}(r)$ function, random labeling
519 the cases (medium and high degrees) and controls (absent or low degree) of
520 Fe-Mn oxides on the lithic and faunal assemblages from SU C. The empirical
521 values of the cross-type function are balanced on the theoretical expectation
522 for complete spatial independence (red line). It clearly lies inside the grey
523 envelope of significance. Therefore, our analysis shows an independent spatial
524 distribution of Fe-Mn patinated and non-patinated lithic artifacts and fossils
525 from SU C. In the lower unit (SU D), where figure 4b indicates higher density
526 of oxidized artifacts, estimations of the cross-type K function suggests that they
527 occur closer than expected to fresh ones.

528 7. Discussion

529 The Early Pleistocene site of Pirro Nord (fissure P13) has yielded evidence
530 for one of the earliest occurrences of hominins in Europe. The importance of the
531 evidence calls for a multivariate taphonomic analysis in order to establish the
532 nature of the processes involved in the formation of the deposit and the degree
533 of its post-depositional disturbance. We address that need by investigating the
534 spatial association of the archaeological and paleontological remains, as well as
535 the spatial distribution of artifacts and fossils with diagenetic alterations. We
536 focused our analysis on the lower stratigraphic units C and D, since they provide
537 the most significant corpus of finds and they have been studied with the same
538 research protocol.

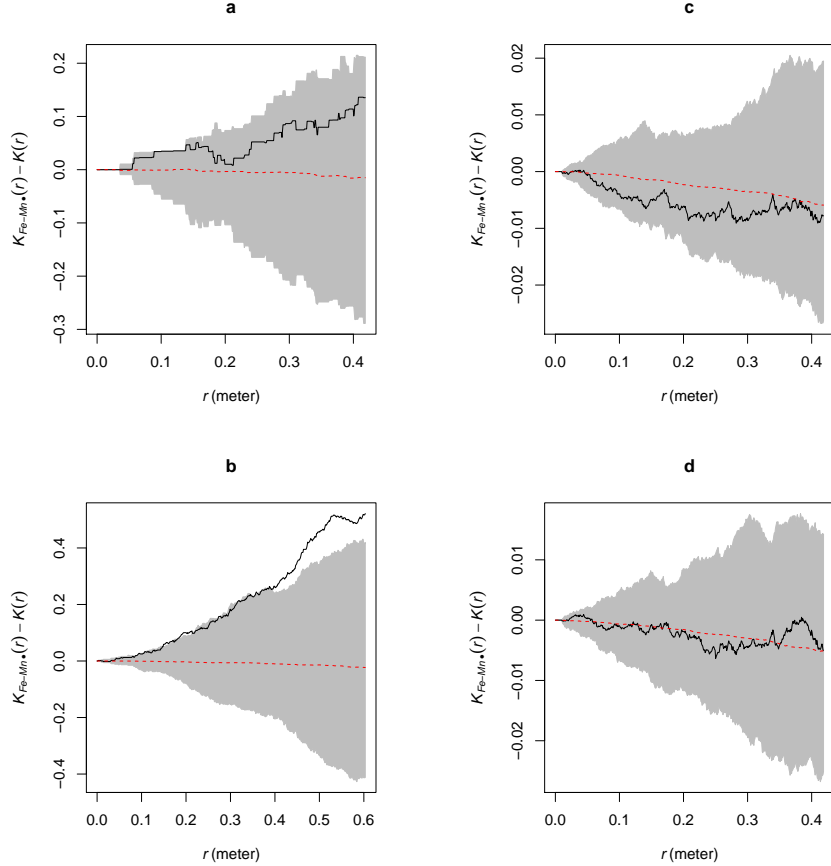


Figure 9: Pointwise envelopes of the homogeneous bivariate $K_{ij}(r)$ function, random labeling cases/*controls* of patinated lithics in SU's C (a) and D (b); oxidized fossils in SU C (c); Fe-Mn oxides on the lithic and the faunal assemblage from SU C (d).

539 *7.1. Formation processes*

540 Non-parametric analyses have been carried out in order to characterize the
541 processes responsible for the formation of the deposit. Then, we accounted for
542 the relative spatial pattern of the different types of finds.

543 The vertical distribution of the archaeological and paleontological assem-
544 blages does not appear to be affected by strong gravitational effects. On the
545 other hand, it resemble a 'nearly' normal distribution and suggests a very close
546 mean occurrence of lithic artifacts and *A. ruffoi* remains, despite the small sam-
547 ple of micromammals (Fig. 3). A visual interpretation of the projected third
548 coordinate (Fig. 5a,b) also suggests that the intensity of finds is not a function
549 of the covariate z . Moreover, higher densities are not linked to the thickness of
550 the stratigraphic units. They are clearly localized at values of $6 < x < 7$ and
551 $8 < x < 9$ in both the SU's, as showed also by figures 5c,d and 6a,d. Indeed,
552 the Berman's Z_2 test for the dependence of the point process on the spatial co-
553 variate x failed to reject the null hypothesis for SU C ($p-value = 0.00445$) and
554 D ($p-value = 1.913e - 14$). However, even if it suggests significant evidence
555 that the intensity depends on some covariate, the effect of that covariate could
556 still be weak. ROC curves (Fig. 5e,f) indicate that the x coordinate does not
557 have discriminatory power.

558 Bartlett (1963) showed that it is possible to formulate a point pattern which
559 can be equally interpreted as a Poisson inhomogeneous process, or a homoge-
560 neous cluster process. According to our non-parametric analyses, we proceeded
561 under the assumption that the processes involved in the formation of the Pirro
562 Nord (P13) deposit are homogeneous and clustered. The scan tests in figures
563 6a,d show hot spots of points, mostly localized between $6 < x < 7$ and $8 < x < 9$.
564 The cluster correlation between all the finds is significantly confirmed by the
565 estimations of the K and F functions (Fig. 6). The first lines of panels in figures
566 7 and 8 offer a type-based view of these patterns. Indeed, the estimated $\hat{K}(r)$
567 functions of the faunal assemblage (Fig. 7a and 8a), which constitute the big-
568 ger part of the analyzed sample of data, resemble the results for the complete
569 populations (Fig. 6b,e). The lithic assemblage also show significat aggregation;

⁵⁷⁰ while the small sample of *A. ruffoi* falls inside the envelope of CSR.

⁵⁷¹ Faunal remains and lithic artifacts show some overlapping when evaluated
⁵⁷² by means of Gaussian smoothing kernel (Fig. 5c,d). Positive spatial association
⁵⁷³ between fossils and lithics is statistically confirmed by the cross-type *K* and *G*
⁵⁷⁴ functions for the examined SU's (Fig. 7 and 8). Fossils and artifacts tend
⁵⁷⁵ then to occur aggregated with each other (they are closest than expected for
⁵⁷⁶ a independent process). Significant spatial proximity is also showed between
⁵⁷⁷ artifacts and micromammal remains, especially in SU D.

⁵⁷⁸ According to the results of our analyses, the stratigraphic and spatial as-
⁵⁷⁹ sociation between the types of remains should be considered as the result of
⁵⁸⁰ the same formation process. Finds occur in the clayey-sand sediment together
⁵⁸¹ with a high number of angular to sub-rounded gravels and boulder-sized rock
⁵⁸² clasts. Such a stratigraphic setting suggests repeated mass-wasting processes
⁵⁸³ (at least two events, represented by SU's C and D, which were included in this
⁵⁸⁴ study) with low degree of reworking in a relatively short span of time (Arzarello
⁵⁸⁵ et al., 2012). Rapid-moving and chaotic water-laden masses, such as mud-flows
⁵⁸⁶ or earth-flows, of soilwash and rock rubble with fossils and artifacts (Butzer,
⁵⁸⁷ 1982, p. 46), could have been triggered by intense rainfalls and trapped in the
⁵⁸⁸ karst sink-hole directly opening to the outside. Sedimentary filling would have
⁵⁸⁹ derived from the top, by gravity, directed into the empty space between the
⁵⁹⁰ large limestone blocks that made up the internal structure of the fissure. The
⁵⁹¹ thickness of the layers is likely correlated to the intensity of such events.

⁵⁹² On the other hand, the clustered distribution of all the finds cannot be linked
⁵⁹³ to the thickness of the statigraphic units. The big blocks of calcarenite, which in
⁵⁹⁴ some places transect the stratigraphic units (Fig. 1), created a complex internal
⁵⁹⁵ structure and might have influenced the direction of sediment accumulation.
⁵⁹⁶ However, sedimentation rate, driven by the rugged topography of the site, does
⁵⁹⁷ not seem to be spatially associated with the localized hot spots (Fig. 6a,d).
⁵⁹⁸ Thus, clustering might have been a correlated effect of the formation process.

⁵⁹⁹ The presence of partially articulated vertebrate skeletal elements and their
⁶⁰⁰ general low degree of weathering indicate fast burial and transport of bones from

601 nearby locations (Bagnus, 2011). A close spatial proximity between the original
602 location of the finds and the karst fissure, as well as a relatively fast burial, is
603 also corroborated by the unrounded ridges and edges of the lithic artifacts and
604 by the technological consistency of the assemblage (Arzarello et al., 2014).

605 In conclusion, our spatial statistics analyses confirm the field observations
606 about the spatial association of archaeological and paleontological remains.

607 *7.2. Post-depositional processes*

608 After dealing with our first research question (to examine the spatial dis-
609 tribution of finds in the context of the site formation processes), our analyses
610 were particularly directed to test the hypothesis of post-depositional processes
611 reworking the deposit. We assume that the spatial aggregation of taphonomic
612 surface alterations, and their relative segregation compared to non-altered finds,
613 would indicate the localized activity of diagenetic agents.

614 We focused more on the spatial distribution of oxides, because traditional
615 explanations for the development of Fe-Mn patinas on the surface of flint refer to
616 the deposition of various iron and manganese oxides and hydroxides out of soil
617 water (Stapert, 1976). Similarly, the origin of manganese coatings on fossils, in
618 karst environments, may derive from circulating water, or from the manganese
619 present in the surrounding limestone rock dissolved by groundwater (Hill, 1982).

620 The vertical distribution of oxides on the lithic artifacts and the sample of
621 faunal remains (Fig. 4) spans the complete stratigraphic sequence and appar-
622 ently shows a gradual increase through the lower layers, especially in the lithics
623 assemblage. Intensity of oxides is indeed more likely proportional to the density
624 of finds and not related to the depth.

625 By applying a set of spatial statistics (namely cross-type $K_{ij}(r)$ function)
626 to the archaeological and paleontological remains, we searched for evidence of
627 localized areas, which might have been subjected to the presence of water, es-
628 pecially water-flows.

629 In SU C, the spatial distribution of Fe-Mn patinas on lithics and fossils
630 is, with a certain degree of significance, the result of independent processes

631 (Fig. 9a,c,d). We cannot state that there is aggregation (spatial proximity)
632 between oxidized finds and fresh ones. Neither the results of the bivariate K
633 function, random labeling the cases/controls of Fe-Mn coating, show segreg-
634 ation, which indicative of spatially defined diagenetic processes. In contrast, in
635 SU D (Fig. 9b), patinated and fresh artifacts occur significantly spatially aggre-
636 gated to each other for values of $r > 0.4m$. They occur closer than expected by
637 an independent process at bigger scale. However, the pattern is, with a certain
638 confidence level, independent.

639 Rottländer (1975) identified a possible different cause of Fe-Mn coatings in
640 the iron that is already present in the flint. In this light, the spatial association
641 of flint artifacts with and without patination also depends on the chemical and
642 microstructural composition of the raw material itself. On the other hand,
643 the same oxides affecting a good percentage of finds, have been equally found
644 broadly scattered on the numerous clasts of calcarenite that are included in the
645 matrix, thus supporting an external origin of the Fe-Mn coating process.

646 The content of water and organic matter in the sedimentary body could be
647 responsible for the randomly diffuse Fe-Mn patinations. In presence of organic
648 matter, indeed, it is likely that the release of organic acids will accelerate pati-
649 nation on chert (Burroni et al., 2002). Moisture of the sedimentary body could
650 also be accounted for the wide random spread of Fe-Mn coatings.

651 We did not find statistically significant evidence of aggregation of oxidized
652 records compared to non-oxidized ones (Fig. 9c); thus, we can exclude the as-
653 sumption of localized concentration of water, which is included in the hypothesis
654 advanced by Bagnus (2011) for the presence of inner flows reworking the deposit.

655 Due to the small sample size, we did not apply spatial analysis to the distri-
656 bution of the three taphorecords. However, figure 4e,f suggests that fossils from
657 the TR1 group occur spatially aggregated with fossils from the TR2 and TR3
658 groups. Considering the distribution of Fe-Mn oxides on the lithic and faunal
659 assemblages, the re-elaborated TR1 (*sensu* Fernández-López, 1991, 2007, 2011)
660 might not be associated with the reworking action of water-flows and might
661 be more likely correlated to random and limited rearrangement of parts of the

662 sedimentary matrix.

663 A possible cause of some localized movement of sediments could be the rock
664 falls from the vault of the karst fissure, during the deposition of SU's C and
665 D. As showed in figure 1, an abrupt increase in the number of boulder-sized
666 rocks is observed within the lower layers. Moreover, rock falls caused most of
667 the post-depositional fractures on the faunal assemblage (Bagnus, 2011). Such
668 intense erosional process could most likely be correlated to the seismic activity
669 of the region (Bertok et al., 2013).

670 Results of our analyses suggest that post-depositional taphonomic alter-
671 ations occurred with a certain significance as result of independent processes.
672 However, keeping a caution approach to spatial analysis, a documented point
673 pattern can be most realistically thought of as the result of multiple processes
674 heterogeneously working at different scales (Bevan and Wilson, 2013). Multi-
675 ple or repeated post-depositional processes could obliterate contemporaneous or
676 preceding patterns, resulting in a final random distribution of the record.

677 Moreover, karst site formation processes are highly dependent on the struc-
678 ture and extension of the overall karsic system, as well on the surrounding
679 environment. The lack of information about the original characteristics of the
680 system and the reduced area of excavation strongly limit the analysis.

681 Furthermore, although the need for considering three dimensional distribu-
682 tions in site formation processes study, spatial point pattern statistics are at
683 the moment not fully equipped to analyze three-dimensional patterns, espe-
684 cially when the study-area corresponds to a three-dimensional volume with a
685 complex shape such as a karsic structure.

686 On the other hand, "one must look to non-spatial evidence to corroborate or
687 disprove theories about spatial processes" (Hodder and Orton, 1976, p. 8). The
688 integration with other taphonomic disciplines reinforces the results of spatial
689 analyses and outline new opportunities for point pattern analyses. As recently
690 remarked (Cobo-Sánchez et al., 2014), taphonomic research should be multi-
691 variate (Domínguez-Rodrigo and Pickering, 2010) and it should include spatial
692 analysis as a heuristic tool in the interpretation of site integrity. This is espe-

⁶⁹³ cially demanding when the research questions deal with past human behaviour
⁶⁹⁴ and even more so when site dating is based on the stratigraphic association of
⁶⁹⁵ artifacts and fossils.

⁶⁹⁶ **8. Conclusions**

⁶⁹⁷ The Early Pleistocene site of Pirro Nord 13 provides evidence of the earliest
⁶⁹⁸ human presence in Western Europe. Lithic artifacts have been found in a karst
⁶⁹⁹ fissure filling, together with late Villafranchian/early Biharian paleontological
⁷⁰⁰ remains.

⁷⁰¹ The main goals of our study were:

- ⁷⁰² 1. to investigate the depositional processes involved in the formation of the
⁷⁰³ deposit and
- ⁷⁰⁴ 2. to assess the degree of any potential post-depositional reworking of the
⁷⁰⁵ archaeological and paleontological remains.

⁷⁰⁶ The integration of spatial point pattern analyses with previous taphonomic
⁷⁰⁷ studies on the faunal and lithic assemblages allowed us to test different hypothe-
⁷⁰⁸ ses of site formation and modification processes.

⁷⁰⁹ On the basis of our analyses,

- ⁷¹⁰ 1. we consider the deposit as the result of subsequent events of some type of
⁷¹¹ mass-wasting process, such as a mud-flow or earth-flow, carrying rock rub-
⁷¹² ble with fossils and artifacts. The applied set of spatial analyses confirm,
⁷¹³ with an adequate level of statistical significance, this assumption, based
⁷¹⁴ on field observations, regarding the spatial association between the finds.
- ⁷¹⁵ 2. Based on our taphonomic point pattern analyses of several diagenetic fea-
⁷¹⁶ tures on the lithic and faunal assemblages, we reject the hypothesis of a
⁷¹⁷ substantial post-depositional reworking and mixture of the sedimentary
⁷¹⁸ deposit and we corroborate the stratigraphic integrity of the Pirro Nord
⁷¹⁹ 13 site.

Finally, the present study answers the need for a taphonomic perspective in spatial analysis, by applying well developed quantitative methods in spatial statistics. Point pattern analysis can be very flexible and useful in the investigation of both cultural and taphonomic processes. Until now it has found limited application on taphonomic studies, but, as our study demonstrates, it offers new analytical opportunities to the multidisciplinary study of the complex processes that operate in the formation and modification of archaeological sites. It allows analysts to test multiscalar patterns and to model the taphonomic processes underlying archaeological distributions, which are otherwise difficult to identify from the simple visualization of maps, especially for those sites characterized by complex geo-stratigraphic settings.

Acknowledgements

DG was supported by the European Research Council Starting Grant PaGE, No. 283503.

Fieldworks were financially supported by the University of Ferrara and the Apricena Municipality. Excavations were possible thanks to the concession by the Soprintendenza Archeologica della Puglia and Ministero dei Beni e delle Attività Culturali; and thanks to the collaboration of Dott.ssa Anna Maria Tunzi. Excavations were also possible thanks to the kind disposability of Gaetano and Franco dell’Erba.

We would like to thank all those who attended the excavation campaigns for their indispensable cooperation; Julie Arnaud for her contribution to the 3D modeling of the site; Nick Thompson for English proofreading.

We are grateful to Vangelis Tourloukis and two anonymous reviewers for critical discussions and many constructive comments that helped to improve this manuscript.

⁷⁴⁶ **References**

- ⁷⁴⁷ Anderson, K. L., Burke, A., 2008. Refining the definition of cultural levels at
⁷⁴⁸ Karabi Tamchin: a quantitative approach to vertical intra-site spatial analy-
⁷⁴⁹ sis. *Journal of Archaeological Science* 35 (8), 2274–2285.
- ⁷⁵⁰ Arzarello, M., Marcolini, F., Pavia, G., Pavia, M., Petronio, C., Petrucci, M.,
⁷⁵¹ Rook, L., Sardella, R., 2007. Evidence of earliest human occurrence in Europe:
⁷⁵² the site of Pirro Nord (Southern Italy). *Naturwissenschaften* 94, 107–112.
- ⁷⁵³ Arzarello, M., Marcolini, F., Pavia, G., Pavia, M., Petronio, C., Petrucci, M.,
⁷⁵⁴ Rook, L., Sardella, R., 2009. L'industrie lithique du site Pléistocène inférieur
⁷⁵⁵ de Pirro Nord (Apricena, Italie du sud): une occupation humaine entre 1,3
⁷⁵⁶ et 1,7 Ma. *L'Anthropologie* 113 (1), 47–58.
- ⁷⁵⁷ Arzarello, M., Pavia, G., Peretto, C., Petronio, C., Sardella, R., 2012. Evidence
⁷⁵⁸ of an Early Pleistocene hominin presence at Pirro Nord (Apricena, Foggia,
⁷⁵⁹ southern Italy): P13 site. *Quaternary International* 267, 56–61.
- ⁷⁶⁰ Arzarello, M., Peretto, C., 2010. Out of Africa: The first evidence of Italian
⁷⁶¹ peninsula occupation. *Quaternary International* 223–224, 65–70.
- ⁷⁶² Arzarello, M., Peretto, C., Moncel, M.-H., 2014. The Pirro Nord site (Apricena,
⁷⁶³ Fg, Southern Italy) in the context of the first European peopling: Conver-
⁷⁶⁴ gences and divergences. *Quaternary International In Press*.
- ⁷⁶⁵ Baddeley, A., Rubak, E., Turner, R., 2015. Spatial Point Patterns: Methodology
⁷⁶⁶ and Applications with R, in press Edition. Chapman and Hall/CRC Press,
⁷⁶⁷ London.
- ⁷⁶⁸ Bagnus, C., 2011. Analisi tafonomica delle associazione a vertebrati del Pleis-
⁷⁶⁹ tocene Inferiore di Pirro Nord. Ph.D. thesis, Università degli Studi di Torino,
⁷⁷⁰ Italy.
- ⁷⁷¹ Bailey, T., Gatrell, A., 1995. Interactive spatial data analysis. Longman Scien-
⁷⁷² tific and Technical, Harlow Essex, England.

- ⁷⁷³ Bartlett, M. S., 1963. The spectral analysis of point processes. *Journal of the
774 Royal Statistical Society, Series B* 29, 264–296.
- ⁷⁷⁵ Behrensmeyer, A. K., 1978. Taphonomic and ecologic information from bone
776 weathering. *Paleobiology* 4 (2), 150–162.
- ⁷⁷⁷ Behrensmeyer, A. K., 1991. Terrestrial vertebrate accumulations. In: Allison,
778 Briggs, D. (Eds.), *Taphonomy: Releasing the Data Locked in the Fossil
779 Record: Topics in Geobiology*. Vol. 9. Plenum Press, New York, p. 291–327.
- ⁷⁸⁰ Benito-Calvo, A., de la Torre, I., 2011. Analysis of orientation patterns in Oldu-
781 vau Bed I assemblages using GIS techniques: Implications for site formation
782 processes. *Journal of Human Evolution* 61 (1), 50–60.
- ⁷⁸³ Bernatchez, J. A., 2010. Taphonomic implications of orientation of plotted finds
784 from Pinnacle Point 13B (Mossel Bay, Western Cape Province, South Africa).
785 *Journal of Human Evolution* 59 (3–4), 274–288.
- ⁷⁸⁶ Bertok, C., Masini, F., Donato, V. D., Martire, L., Pavia, M., Zunino, M.,
787 Pavia, G., 2013. Stratigraphic framework of the type-locality of Pirro Nord
788 mammal Faunal Unit (Late Villafranchian, Apricena, south- eastern Italy).
789 *Palaeontographica* 298 (6), 5–17.
- ⁷⁹⁰ Bertran, P., Hetù, B., Texier, J.-P., Steijn, H. V., 1997. Fabric characteristics
791 of subaerial slope deposits. *Sedimentology* 44 (1), 1–16.
- ⁷⁹² Bertran, P., Lenoble, A., Todisco, D., Desrosiers, P. M., Sørensen, M., 2012.
793 Particle size distribution of lithic assemblages and taphonomy of Palaeolithic
794 sites. *Journal of Archaeological Science* 39 (10), 3148–3166.
- ⁷⁹⁵ Bertran, P., Texier, J.-P., 1995. Fabric Analysis: Application to Paleolithic
796 Sites. *Journal of Archaeological Science* 22 (4), 521–535.
- ⁷⁹⁷ Bertran, P., Émilie Claud, Detrain, L., Lenoble, A., Masson, B., Vallin, L., 2006.
798 Composition granulométrique des assemblages lithiques, application à l'étude
799 taphonomique des sites paléolithiques. *Paléo* 18, 7–36.

- 800 Bevan, A., Conolly, J., 2006. Multiscalar approaches to settlement pattern anal-
801 ysis. In: Lock, G., Molyneaux, B. (Eds.), *Confronting Scale in Archaeology:*
802 *Issues of Theory and Practice*. Springer, New York, pp. 217–234.
- 803 Bevan, A., Conolly, J., 2009. Modelling spatial heterogeneity and nonstation-
804 arity in artifact-rich landscapes. *Journal of Archaeological Science* 36 (4),
805 956–964.
- 806 Bevan, A., Conolly, J., 2013. *Mediterranean Islands, Fragile Communities and*
807 *Persistent Landscapes: Antikythera in Long-term Perspective*. Cambridge
808 University Press, Cambridge.
- 809 Bevan, A., Crema, E., Li, X., Palmisano, A., 2013. Intensities, interactions,
810 and uncertainties: Some new approaches to archaeological distributions. In:
811 Bevan, A., Lake, M. (Eds.), *Computational Approaches to Archaeological*
812 *Spaces*. Left Coast Press, Walnut Creek, pp. 27–52.
- 813 Bevan, A., Wilson, A., 2013. Models of settlement hierarchy based on partial
814 evidence. *Journal of Archaeological Science* 40 (5), 2415–2427.
- 815 Burroni, D., Donahue, R. E., Pollard, A., Mussi, M., 2002. The surface alteration
816 features of flint artefacts as a record of environmental processes. *Journal of*
817 *Archaeological Science* 29 (11), 1277–1287.
- 818 Butzer, K., 1982. *Archaeology as Human Ecology: Method and Theory for a*
819 *Contextual Approach*. Cambridge University Press, New York.
- 820 Carbonell, E., Bermudez de Castro, J. M., Pares, J. M., Perez-Gonzalez, A.,
821 Cuenca-Bescos, G., Olle, A., Mosquera, M., Huguet, R., van der Made, J.,
822 Rosas, A., Sala, R., Vallverdu, J., Garcia, N., Granger, D. E., Martinon-
823 Torres, M., Rodriguez, X. P., Stock, G. M., Verges, J. M., Allue, E., Burjachs,
824 F., Caceres, I., Canals, A., Benito, A., Diez, C., Lozano, M., Mateos, A.,
825 Navazo, M., Rodriguez, J., Rosell, J., Arsuaga, J. L., 2008. The first hominin
826 of Europe. *Nature* 452, 465–469.

- 827 Carrer, F., 2015. Interpreting intra-site spatial patterns in seasonal contexts: an
828 ethnoarchaeological case study from the western alps. *Journal of Archaeological*
829 *Method and Theory*, 1–25.
- 830 Cobo-Sánchez, L., Aramendi, J., Domínguez-Rodrigo, M., 2014. Orientation
831 patterns of wildebeest bones on the lake Masek floodplain (Serengeti, Tan-
832 zania) and their relevance to interpret anisotropy in the Olduvai lacustrine
833 floodplain. *Quaternary International* 322–323 (0), 277–284.
- 834 Crema, E. R., 2015. Time and probabilistic reasoning in settlement analysis.
835 In: Juan A. Barcelo, I. B. (Ed.), *Mathematics and Archaeology*. CRC Press,
836 Boca Raton, FL, pp. 314–334.
- 837 Crema, E. R., Bevan, A., Lake, M. W., 2010. A probabilistic framework for
838 assessing spatio-temporal point patterns in the archaeological record. *Journal*
839 *of Archaeological Science* 37 (5), 1118–1130.
- 840 Crema, E. R., Bianchi, E., 2013. Looking for patterns in the noise: non-site
841 spatial-analysis in Sebkha Kelbia. In: Mulazzani, S. (Ed.), *Le Capsien de*
842 *herglia (Tunisie). Culture, environnement et économie*. Africa Magna Verlag,
843 Frankfurt, pp. 385–395.
- 844 Crochet, J.-Y., Welcomme, J.-L., Ivorra, J., Ruffet, G., Boulbes, N., Capdevila,
845 R., Claude, J., Firmat, C., Métais, G., Michaux, J., Pickford, M., 2009. Une
846 nouvelle faune de vertébrés continentaux, associée à des artefacts dans le
847 Pléistocène inférieur de l'Hérault (Sud de la France), vers 1,57 Ma. *Comptes*
848 *Rendus Palevol* 8 (8), 725–736.
- 849 de la Torre, I., Benito-Calvo, A., 2013. Application of GIS methods to retrieve
850 orientation patterns from imagery; a case study from Beds I and II, Olduvai
851 Gorge (Tanzania). *Journal of Archaeological Science* 40 (5), 2446–2457.
- 852 Despriée, J., Gageonnet, R., Voinchet, P., Bahain, J.-J., Falguères, C., Varache,
853 F., Courcimault, G., Dolo, J.-M., 2006. Une occupation humaine au Pléis-

- 854 tocène inférieur sur la bordure nord du Massif central. Comptes Rendus
855 Palevol 5 (6), 821–828.
- 856 Despriée, J., Voinchet, P., Gageonnet, R., Dépont, J., Bahain, J.-J., Falguères,
857 C., Tissoux, H., Dolo, J.-M., Courcimault, G., 2009. Les vagues de peuplement
858 humains au Pléistocène inférieur et moyen dans le bassin de la Loire
859 moyenne, région Centre, France. Apports de l'étude des formations fluviatiles.
860 L'Anthropologie 113 (1), 125–167.
- 861 Despriée, J., Voinchet, P., Tissoux, H., Moncel, M.-H., Arzarello, M., Robin,
862 S., Bahain, J.-J., Falguères, C., Courcimault, G., Dépont, J., Gageonnet,
863 R., Marquer, L., Messager, E., Abdessadok, S., Puaud, S., 2010. Lower and
864 middle Pleistocene human settlements in the Middle Loire River Basin, Centre
865 Region, France. Quaternary International 223–224, 345–359.
- 866 Dibble, H. L., Chase, P. G., McPherron, S. P., Tuffreau, A., Oct. 1997. Testing
867 the reality of a "living floor" with archaeological data. American Antiquity
868 62 (4), 629–651.
- 869 Diggle, P., 1985. A kernel method for smoothing point process data. Applied
870 Statistics (Journal of the Royal Statistical Society, Series C) 34, 138–147.
- 871 Diggle, P., 2003. Statistical analysis of spatial point patterns. Hodder Arnold,
872 London.
- 873 Djindjian, F., 1999. L'analyse spatiale de l'habitat: un état de l'art. Archeologia
874 e Calcolatori X, 17–32.
- 875 Domínguez-Rodrigo, M., Bunn, H., Mabulla, A., Baquedano, E., Uribelarrea,
876 D., Pérez-González, A., Gidna, A., Yravedra, J., Diez-Martin, F., Egeland,
877 C., Barba, R., Arriaza, M., Organista, E., Ansón, M., 2014a. On meat eating
878 and human evolution: A taphonomic analysis of BK4b (Upper Bed II, Olduvai
879 Gorge, Tanzania), and its bearing on hominin megafaunal consumption.
880 Quaternary International 322–323, 129–152.

- 881 Domínguez-Rodrigo, M., Diez-Martín, F., Yravedra, J., Barba, R., Mabulla, A.,
882 Baquedano, E., Uribelarrea, D., Sánchez, P., Eren, M. I., 2014b. Study of the
883 SHK Main Site faunal assemblage, Olduvai Gorge, Tanzania: Implications
884 for Bed II taphonomy, paleoecology, and hominin utilization of megafauna.
885 Quaternary International 322–323, 153–166.
- 886 Domínguez-Rodrigo, M., Fernández-López, S., Alcalá, L., 2011. How Can
887 Taphonomy Be Defined in the XXI Century? Journal of Taphonomy 9 (1),
888 1–13.
- 889 Domínguez-Rodrigo, M., Pickering, T., 2010. A multivariate approach for dis-
890 criminating bone accumulations created by spotted hyenas and leopards: har-
891 nessing actualistic data from east and southern Africa. Journal of Taphonomy
892 8 (2-3), 155–179.
- 893 Domínguez-Rodrigo, M., Uribelarrea, D., Santonja, M., Bunn, H., García-Pérez,
894 A., Pérez-González, A., Panera, J., Rubio-Jara, S., Mabulla, A., Baquedano,
895 E., Yravedra, J., Diez-Martín, F., 2014c. Autochthonous anisotropy of ar-
896 chaeological materials by the action of water: experimental and archaeolog-
897 ical reassessment of the orientation patterns at the Olduvai sites. Journal of
898 Archaeological Science 41, 44–68.
- 899 Díez, J. C., Fernández-Jalvo, J., Rossel, J., Cáceres, I., 1999. Zooarchaeology
900 and taphonomy of Aurora Stratum (Gran Dolina, Sierra de Atapuerca, Spain).
901 Journal of Human Evolution 37, 623–652.
- 902 Efremov, I. A., 1940. Taphonomy: a new branch of paleontology. Pan American
903 Geologist 74, 81–93.
- 904 Eve, S. J., Crema, E. R., 2014. A House with a View? Multi-model inference,
905 visibility fields, and point process analysis of a Bronze Age settlement on
906 Leskernick Hill (Cornwall, UK). Journal of Archaeological Science 43, 267–
907 277.

- ⁹⁰⁸ Fernández-López, S. R., 2000. Temas de Tafonomía. Departamento de Paleon-
- ⁹⁰⁹ tología, Universidad Complutense de Madrid.
- ⁹¹⁰ Fernández-López, S. R., 1987. Unidades registráticas, biocronología y
- ⁹¹¹ geocrontología. Revista Española de Paleontología 2, 65–85.
- ⁹¹² Fernández-López, S. R., 1991. Taphonomic concepts for a theoretical biochronol-
- ⁹¹³ ogy. Revista Española de Paleontología 6, 37–49.
- ⁹¹⁴ Fernández-López, S. R., 2007. Ammonoid taphonomy, palaeoenvironments and
- ⁹¹⁵ sequence stratigraphy at the Bajocian/Bathonian boundary on the Bas Auran
- ⁹¹⁶ area (Subalpine Basin, SE France). Lethaia 40, 377–391.
- ⁹¹⁷ Fernández-López, S. R., 2011. Taphonomic analysis and sequence stratigraphy
- ⁹¹⁸ of the Albarracinites beds (lower Bajocian, Iberian Range, Spain). An exam-
- ⁹¹⁹ ple of shallow condensed section. Bulletin de la Société Géologique de France
- ⁹²⁰ 182, 405–415.
- ⁹²¹ Gatrell, A. C., Bailey, T. C., Diggle, P. J., Rowlingson, B. S., 1996. Spatial point
- ⁹²² pattern analysis and its application in geographical epidemiology. Transactions
- ⁹²³ of the Institute of British Geographers 21, 256–274.
- ⁹²⁴ Goreaud, F., Pélissier, R., October 2003. Avoiding misinterpretation of biotic
- ⁹²⁵ interactions with the intertype k_{12} -function: population independence vs. ran-
- ⁹²⁶ dom labelling hypotheses. Journal of Vegetation Science 14 (5), 681–692.
- ⁹²⁷ Hill, C. A., 1982. Origin of black deposits in caves. National Speleological Society
- ⁹²⁸ Bulletin 44, 15–19.
- ⁹²⁹ Hodder, I., Orton, C., 1976. Spatial Analysis in Archaeology. New Studies in
- ⁹³⁰ Archaeology. Cambridge University Press, Cambridge.
- ⁹³¹ Kos, A. M., 2003. Characterization of post-depositional taphonomic processes
- ⁹³² in the accumulation of mammals in a pitfall cave deposit from southeastern
- ⁹³³ Australia. Journal of Archaeological Science 30, 781–796.

- 934 Lenoble, A., Bertran, P., 2004. Fabric of Palaeolithic levels: methods and impli-
935 cations for site formation processes. Journal of Archaeological Science 31 (4),
936 457–469.
- 937 Lopez-García, J. M., Luzi, E., Berto, C., Peretto, C., Arzarello, M., 2015.
938 Chronological context of the first hominin occurrence in southern Europe:
939 the *Allophaiomys ruffoi* (Arvicolinae, Rodentia, Mammalia) from Pirro 13
940 (Pirro Nord, Apulia, southwestern Italy). Quaternary Science Reviews 107,
941 260–266.
- 942 Lumley, H., Krzepkowska, A., Echassoux, A., 1988. L'industrie du Pleistocene
943 inférieur de la grotte du Vallonnet, Roquebrune-Cap Martin, Alpes Maritimes.
944 L'Anthropologie 92, 501–614.
- 945 López-González, F., Grandal-d'Anglade, A., Vidal-Romaní, J. R., 2006. Deci-
946 phering bone depositional sequences in caves through the study of manganese
947 coatings. Journal of Archaeological Science 33 (5), 707–717.
- 948 López-Ortega, E., Rodríguez, X. P., Vaquero, M., 2011. Lithic refitting and
949 movement connections: the NW area of level TD10-1 at the Gran Dolina
950 site (Sierra de Atapuerca, Burgos, Spain). Journal of Archaeological Science
951 38 (11), 3112–3121.
- 952 McPherron, S. J., 2005. Artifact orientations and site formation processes from
953 total station proveniences. Journal of Archaeological Science 32 (7), 1003–
954 1014.
- 955 Ohser, J., 1983. On estimators for the reduced second moment measure of point
956 processes. Mathematische Operationsforschung und Statistik, series Statistics
957 14, 63–71.
- 958 Openshaw, S., 1996. Developing GIS-relevant zone-based spatial analysis meth-
959 ods. In: Longley, P., Batty, M. (Eds.), Spatial analysis: modelling in a GIS
960 environment. Geoinformation International, London, pp. 55–73.

- ⁹⁶¹ Ord, J. K., 1972. Density estimation and tests for randomness, using distance
⁹⁶² methods. Draft for lecture to Advanced Institute on statistical ecology in the
⁹⁶³ United States, The Pennsylvania State University, (Mimeo).
- ⁹⁶⁴ Orton, C., 1982. Stochastic process and archaeological mechanism in spatial
⁹⁶⁵ analysis. *Journal of Archaeological Science* 9 (1), 1–23.
- ⁹⁶⁶ Orton, C., 2004. Point pattern analysis revisited. *Archeologia e Calcolatori* 15,
⁹⁶⁷ 299–315.
- ⁹⁶⁸ Parés, J. M., Pérez-González, A., Rosas, A., Benito, A., de Castro, J. B., Car-
⁹⁶⁹ bonell, E., Huguet, R., 2006. Matuyama-age lithic tools from the Sima del
⁹⁷⁰ Elefante site, Atapuerca (northern Spain). *Journal of Human Evolution* 50 (2),
⁹⁷¹ 163–169.
- ⁹⁷² Petraglia, M. D., Nash, D. T., 1987. The impact of fluvial processes on experi-
⁹⁷³ mental sites. In: Nash, D. T., Petraglia, M. D. (Eds.), *Natural formation pro-*
⁹⁷⁴ *cesses and the archaeological record*. Vol. 352 of *International Series. British*
⁹⁷⁵ *Archaeological Reports*, Oxford, pp. 108–130.
- ⁹⁷⁶ Petraglia, M. D., Potts, R., 1994. Water Flow and the Formation of Early Pleis-
⁹⁷⁷ tocene Artifact Sites in Olduvai Gorge, Tanzania. *Journal of Anthropological*
⁹⁷⁸ *Archaeology* 13 (3), 228–254.
- ⁹⁷⁹ R Core Team, 2015. R: A Language and Environment for Statistical Computing.
⁹⁸⁰ R Foundation for Statistical Computing, Vienna, Austria.
- ⁹⁸¹ Ripley, B., 1988. Statistical inference for spatial processes. Cambridge University
⁹⁸² Press.
- ⁹⁸³ Ripley, B. D., 1976. The second-order analysis of stationary point processes.
⁹⁸⁴ *Journal of Applied Probability* 13 (2), 255–266.
- ⁹⁸⁵ Ripley, B. D., 1977. Modelling spatial patterns. *Journal of the Royal Statistical*
⁹⁸⁶ *Society, series B* 39, 172–212.

- 987 Robert, C., Casella, G., 2004. Monte Carlo Statistical Methods, second edition
988 Edition. Springer Texts in Statistics. Springer New York, New York.
- 989 Rottländer, R., 1975. The formation of patina on flint. *Archaeometry* 17 (1),
990 106–110.
- 991 Schick, K. D., 1984. Processes of Paleolithic site formation: an experimental
992 study. Ph.D. thesis, University of California, Berkeley, US.
- 993 Schick, K. D., 1986. Stone Age sites in the making: experiments in the formation
994 and transformation of archaeological occurrences. Vol. 319 of International
995 Series. British Archaeological Reports, Oxford.
- 996 Schiffer, M. B., 1972. Archaeological Context and Systemic Context. *American
997 Antiquity* 37 (2), 156–165.
- 998 Schiffer, M. B., 1983. Toward the identification of formation processes. *American
999 Antiquity* 48 (4), 675–706.
- 1000 Schiffer, M. B., 1987. Formation processes of the archaeological record. University
1001 of New Mexico Press, Albuquerque.
- 1002 Sisk, M. L., Shea, J. J., 2008. Intrasite spatial variation of the Omo Kibish
1003 Middle Stone Age assemblages: Artifact refitting and distribution patterns.
1004 *Journal of Human Evolution* 55 (3), 486–500.
- 1005 Stapert, D., 1976. Some natural surface modifications on chert in the Nether-
1006 lands. *Palaeohistoria* 18, 7–41.
- 1007 Texier, J.-P., 2000. A propos des processus de formation des sites préhistoriques
1008 / About prehistoric site formation processes. *Paléo* 12 (1), 379–386.
- 1009 Tobler, W. R., 1970. A computer movie simulating urban growth in the Detroit
1010 region. *Economic Geography* 46 (2), 234–240.
- 1011 Toro-Moyano, I., Barsky, D., Cauche, D., Celiberti, V., Grégoire, S., Lebegue,
1012 F., Moncel, M. H., de Lumley, H., 2011. The archaic stone tool industry from

- ¹⁰¹³ Barranco León and Fuente Nueva 3, (Orce, Spain): Evidence of the earliest
¹⁰¹⁴ hominin presence in southern Europe. *Quaternary International* 243 (1), 80–
¹⁰¹⁵ 91.
- ¹⁰¹⁶ Toro-Moyano, I., de Lumley, H., Fajardo, B., Barsky, D., Cauche, D., Celiberti,
¹⁰¹⁷ V., Grégoire, S., Martinez-Navarro, B., Espigares, M. P., Ros-Montoya, S.,
¹⁰¹⁸ 2009. L’industrie lithique des gisements du Pléistocène inférieur de Barranco
¹⁰¹⁹ León et Fuente Nueva 3 à Orce, Grenade, Espagne. *L’Anthropologie* 113 (1),
¹⁰²⁰ 111–124.
- ¹⁰²¹ Toro-Moyano, I., Martínez-Navarro, B., Agustí, J., Souday, C., de Castro, J. B.,
¹⁰²² Martinón-Torres, M., Fajardo, B., Duval, M., Falguères, C., Oms, O., Parés,
¹⁰²³ J., Anadón, P., Julià, R., García-Aguilar, J., Moigne, A.-M., Espigares, M.,
¹⁰²⁴ Ros-Montoya, S., Palmqvist, P., 2013. The oldest human fossil in Europe,
¹⁰²⁵ from Orce (Spain). *Journal of Human Evolution* 65 (1), 1–9.
- ¹⁰²⁶ Torres, T., Ortiz, J. E., Cobo, R., 2003. Features of deep cave sediments: their
¹⁰²⁷ influence on fossil preservation. *Estudios Geológico* 59, 195–204.
- ¹⁰²⁸ Villa, P., 1982. Conjoinable Pieces and Site Formation Processes. *American
1029 Antiquity* 47 (2), 276–290.
- ¹⁰³⁰ Whallon, R. J., 1974. Spatial analysis of occupation floors ii: The application
¹⁰³¹ of nearest neighbor analysis. *American Antiquity* 39 (1), 16–34.
- ¹⁰³² White, W. B., 1976. Cave minerals and speleothems. In: Ford, T., Cullingford,
¹⁰³³ C. (Eds.), *The Science of Speleology*. Academic Press, London, pp. 267–327.
- ¹⁰³⁴ White, W. B., Vito, C., Scheetz, B. E., 2009. The mineralogy and trace element
¹⁰³⁵ chemistry of black manganese oxide deposits from caves. *Journal of Cave and
1036 Karst Studies* 71 (2), 136–143.
- ¹⁰³⁷ Wood, R. W., Johnson, D. L., 1978. A survey of disturbance processes in archaeo-
¹⁰³⁸ logical site formation. In: Schiffer, M. B. (Ed.), *Advances in archaeological
1039 method and theory*. Vol. 1. Academic Press, New York, Ch. 9, pp. 315–381.